약학석사 학위논문

Structural and Functional Studies on MazF from *Bacillus cereus*

바실러스 세레우스균에서 유래한 MazF 단백질의 구조 및 기능 연구

2021년 1월

서울대학교 대학원

약학과 물리약학전공

김 창 민

Structural and Functional Studies on MazF from *Bacillus cereus*

지도교수 이 봉 진
이 논문을 약학석사 학위논문으로 제출함

2021년 1월

서울대학교 대학원
약학과 물리약학 전공
김 창 민

김창민의 약학석사 학위논문을 인준함
2021년 1월

위 원 장 _____ (인)
부 위 원 장 오규경 (인)
위 원 원 이봉진 (인)

Abstract

Structural and Functional Studies on MazF from *Bacillus cereus*

Kim-Chang Min
College of Pharmacy
Physical Pharmacy
Seoul National University

Toxin–antitoxin (TA) systems are rampant in bacteria and prokaryotes. These systems are known to regulate cellular growth of bacteria in response to stress and other circumstances. The importance of TA systems is largely magnified as various functions have been revealed. In this paper, I presented the crystal structure of BC0266 which is known to as a putative mRNA interferase. And I also reported it as a type II MazF toxin. The MazF toxin is activated during stressful conditions. It cleaves mRNA in a sequence-specific and ribosome-independent manner. Its activated state causes toxic results and may lead to bacterial death. In this study, I experimented structural and functional studies of *Bacillus cereus* and presented the first toxin structure in the TA system of B.cereus. Especially, *B.cereus* MazF adopts a PemK-like fold which is a subfamily of MazF. BC0266 also has an RNA recognizing loops which are called β1–β2 and β3–β4 loops. Key residues of ribonuclease activity are proposed by in vitro assay and mutational studies. It demonstrates the ribonucleic activity and the active sites which are essential for its cellular toxicity.

<Key words>

Toxin-Antitoxin system, MazF type II toxin, *Bacillus cereus,* mRNA interferase, X-ray crystallography

Student Number: 2019-24434

Contents

I. Introduction

1.1. *Bacillus cereus*

1.2. Toxin-Antitoxin system

1.3. Purpose of Research

II. Experimental procedures

2.1. Gene cloning

2.2. Protein expression and purification

2.3. Crystallization and data collection

2.4. Multiple sequence alignment

2.5. In vitro ribonuclease assay

2.6. Site-directed mutagenesis

III. Results
3.1. Gene cloning
3.2. Protein expression and purification
3.3. Crystallization
3.4. Structure of *B.cereus* MazF
3.5. Comparison with MazF homologs
3.6. Functional activity

V.Conclusion

VI.References

국문초록

I. Introduction

1.1. *Bacillus cereus*

Bacillus cereus is a gram-positive bacterium that has recently emerged as a problem of resistance. The virulence factors are enterotoxin and emetic toxin that cause diarrhea and vomiting respectively. It is resistant to heat, acid, and antibiotics and causes a disease called food poisoning. According to a World Health Organization survey, food poisoning kills 420,000 people every year, one-third of which are infants. Especially, more than half of the deaths are caused by diarrhea related to enterotoxin. As such, *B.cereus* is known to be pathogenic, which greatly affects the mortality rate from food poisoning.

Fig. 1. *B.cereus* mortality rate

HAZARD	FOODBORNE ILLNESSES	FOODBORNE DEATHS
TOTAL	600 652 361 (417 646 804-962 834 044)	418 608 (305 128-598 419)
Diarrhoeal disease agents	548 595 679 (369 976 912-888 528 014)	230 111 (160 039-322 359)

Fig. 2. Foodborne deaths by diarrhoeal agents

1.2. Toxin-Antitoxin system

Toxin–antitoxin (TA) systems are prevalent in prokaryotes and function to regulate cellular growth in response to stress such as antibiotic exposure, nutrient starvation, heat shock, and DNA damage. Initially, TA systems were discovered as a part of the plasmid maintenance system, in which only the daughter cells harboring the vertically transferred TA operon can survive. In addition to the primary maintenance function, TA systems are important for bacterial survival. The TA systems are involved in many cellular processes, including cell growth, cell persistence, cell dormancy, biofilm formation, antibiotic resistance, DNA replication, translation, cell division, cell wall synthesis, and cell apoptosis.

TA systems are a two-component system, composed of a toxin and an antitoxin usually sharing the same operon. Currently, TA systems can be categorized into six phenotypes (I-VI) by the nature of each component and the regulatory mechanisms of the antitoxins to its cognate toxins. BC0266(*Bacillus cereus* protein which has 0266 numbering) that I studied belongs to type II system.

Typically, in type II TA system, the rather stable toxins have much more invariant characteristics than their labile and flexible cognate antitoxins. Upon degradation of antitoxins, free toxins can function in postsegregational cell killing, abortive infection, and even bacterial persistence. Thus, it has been regarded that bacterial persistence would indeed be closely related to type II TA systems due to the cellular process-specific nature of type II toxins. One of the best characterized type II toxins is mRNA interferase MazF toxin, belonging to the MazEF family. Comprehensive bioinformatic analyses have shown that MazF is widely distributed in both Gram-positive and Gramnegative bacteria, allowing an in-depth understanding of the consequences of stress and MazF activation on the physiological effects of the bacteria. In addition, understanding of the cutting specificity of MazF on its target RNA is well established. Specifically, the MazF toxin acts as a ribonuclease and cleaves mRNA in a sequence-specific and ribosome-independent manner, but in some cases also cleaves rRNA at specific sequences, exerting its toxicity.

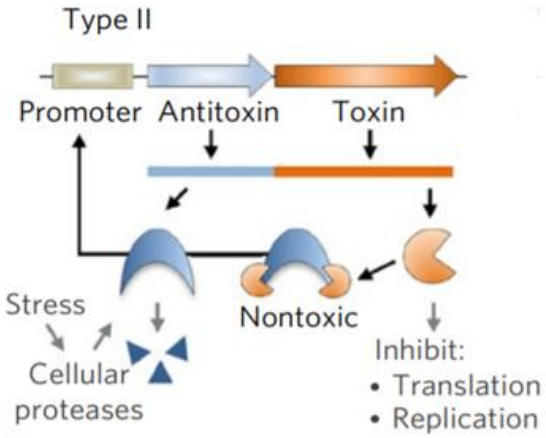

Fig. 3. Mechanism of type II TA system

1.3. Purpose of Research

BC0266 is a *Bacillus cereus* bacterium known to have the function of mRNase interferase. What's interesting is that there has been no known structure in *Bacillus cereus.* The following figure 4 is the list that the pathogens which have been identified in TA proteins so far. If I could identify the structure of BC0266, it has experimental meaning because it was the first structure to be identified by a bacterium called *Bacillus cereus*. So that I started an experiment with the goal of finding out what structure this protein has and actually functions as mRNase.

Determined structure of TA proteins	
Streptococcus pyogenes	*Escherichia coil* O157
Streptococcus pneumonia	*Escherichia coil* K12
Enterococcus faecalis	*Vibrio fischeri*
Staphylococcus aureus	*Brucella abortus*
Neisseria gonorrhoeae	*Salmonella typhimurium*
Rickettsia felis	*Mycobacterium tuberculosis*
Shigella flexneri	*Bacillus subtilis*

Fig. 4. Determined structure of TA proteins

II. Experimental procedures

2.1. Gene cloning

The BC0266 gene was amplified by polymerase chain reaction (PCR). The primers were used in PCR: forward, 5′- GGAATTCCATATGATGATTGTAAAACGCGGC-3′; reverse, 5′-CCGCTCGAGTTAAAAATCTATTAGTCCTAAAC-3′. Restriction enzymes were Nde1 and Xho1. The PCR products and pET28a vector were cut by the same restriction enzymes and ligated to each other. N terminal his tag was attached to the gene of *B. cereus* MazF and was transformed into DH5α competent cell. Lastly, these recombinant plasmids were transformed into E. coli BL21(DE3) competent cells.

2.2. Protein Expression and Purification

Transformed cells were grown in Luria broth (LB) at 37 °C until the OD600 reached to 0.5. The cells were induced by 0.5 mM isopropyl 1-thio-B-D-galactopyranoside (IPTG) for overexpression. And it was incubated for 4 h at 37 °C. These cells were harvested by centrifugation at 6000 rpm. Harvested cells were suspended in a buffer which is 20 mM Tris-HCl, pH 8.0, and 500 mM NaCl(A buffer) containing 5% glycerol and lysed by sonication. Lysed cells were centrifugated for 1 h at 18000 rpm. After centrifugation, the cell debris was discarded and the supernatant was loaded on affinity chromatography using Ni2+ column. Loaded protein was washed with buffer A containing 50 mM imidazole to remove impurities. Then target proteins sticking to the resin was eluted using an imidazole gradient (100−500 mM). Finally, selected high-purity protein was loaded on a size-exclusion chromatography column Superdex 200(GE Healthcare) with final buffer (20 mM Tris, pH 8.0, and 500 mM NaCl). All the purified proteins were assessed by sodium dodecyl sulfate polyacrylamide gel electrophoresis (SDS-PAGE).

2.3. Crystallization and data collection

Crystallization was performed at 293 K by the sitting-drop vapor diffusion method using 96 well crystallization plates. The kinds of crystallization kit were Structure screening (Molecular dimensions), Wizard (Rigaku Reagents) and Index (Hampton Research). Many crystals were created but the only one crystal contained the hit solution which was 100 mM Sodium Citrate, pH 5.6, and 1.0 M ammonium phosphate monobasic. The data were collected using Rayonix MX-300 HE CCD detector at BL44XU of the Spring-8, Japan. The resolution of the hit crystal was 2.00 Å resolution. The structure was phased by single-wavelength anomalous dispersion (SAD) and was refined by SeMet using PHENIX. COOT and PyMOL programs were used for manual model.

2.4. Mutiple Sequence Alignment

There are four MazFs whose structures have been identified. They have similar sequence with *Bacillus cereus* MazF so that I align with them. Alignments of amino acid residues were conducted and the consensus value was 0.85. Percent equivalent was almost same. In visualization, structural information of *B. cereus* MazF was used as top secondary structures and the description and sequence numbering on the topside correspond to *B. cereus* MazF.

2.5. In Vitro Ribonuclease Assay

Ribonuclease assay of *B. cereus* MazF was conducted with an RNase Alert Kit. RNA substrate was interacted with 2 μM, 4 μM, 8 μM, and 16 μM concentrations of *B. cereus* MazF. Then a fluorophore is covalently attached to one end of a synthetic RNA strand and is quenched. The released fluorophore emits fluorescence at 520 nm upon excitation at 490 nm. Assay setting was performed on 384-well opaque plate, and all of experiments were performed in triplicate.

2.6. Site-directed Mutagenesis

Ariginine25 and Threonine 48 which are active residues were mutated to Alanine. Single-site mutations (R25A,T48A) were performed in one step, and double-site mutations(R25A+T48A) were performed in a step-wise manner. All the protocols are conducted by EZchange Site-Directed Mutagenesis Kit. Each plasmid was transformed into E. coli XL10-Gold competent cells and the resulting inserted genes were verified through DNA sequencing.

III. Results

3.1. Gene cloning

Certain sequences of *bacillus cereus* bacteria were amplified by PCR. Histidine tags were attached and inserted into the pet28 vector to obtain recombinant DNA. To see that the recombinant DNA matches the sequence of the original *Bacillus cereus*, I conducted the BLAST and finally confirmed the Align result with 100% Query Cover.

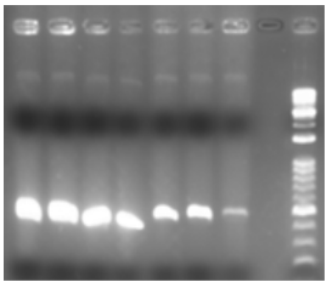

Fig. 5. Gradient PCR of BC0266

3.2. Protein expression and purification

B.cereus MazF was co-expressed in E.coli BL21 (DE3) pLysS and overexpressed after induction by adding IPTG. The heat condition was 37 °C and the incubation time was 4 hours. The protein has high level of expression and solubility. The first step in purification was affinity chromatography. It utilized histidine tag by affinity chromatography on IMAC column which was charged with buffer. The protein was eluted at 100-500 mM imidazole concentration for removing most impurities. The next purification step was size exclusion chromatography. It separates proteins according to their size in order to strip the rest impurities and increase the purity of the target protein.

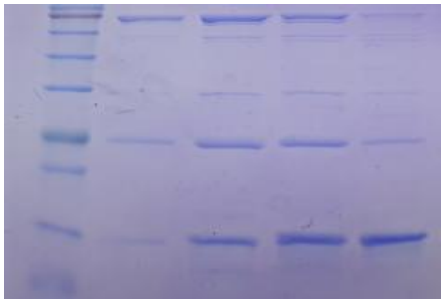

Fig. 6. SDS PAGE of affinity chromatography

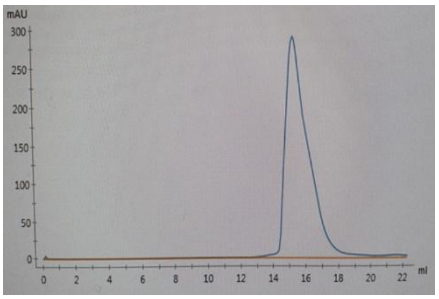

Fig. 7. size exclusion chromatography

3.3. Crystallization

Crystallization was performed at 293 K by the sitting-drop vapor diffusion method in 96 well crystal plates. Two kinds of crystals were obtained which are Native and SeMet. The resolution of Native crystal was 2.0 Å. SeMet crystal was made for resolving phasing problem and its resolution was 2.3 Å. I tried to make crystals in several conditions considering temperature, kinds of reservoir, and buffer etc.

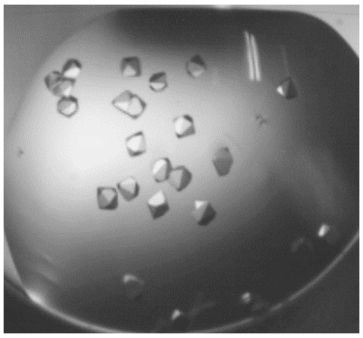

Fig. 8. Native crystal

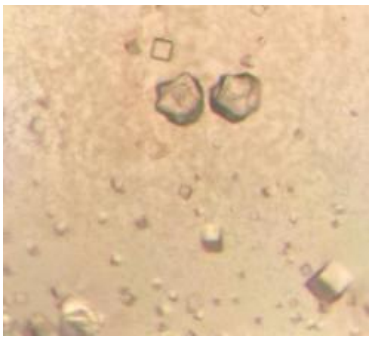

Fig. 9. SeMet crystal

3.4. Structure of *B.cereus* MazF

The structure of *B.cereus* was refined to Rwork factor 18.9% and Rfree factor 22.5%. All amino acids were observed and lie in the Ramachandran plot. Crystals belong to the P3121 space group with the unit cell dimensions of a = b = 60.648 Å, c = 76.247 Å, and α = β = 90.0°, γ = 120°. There are three α-helices and seven β-strands in a monomer state of *B. cereus* MazF. And two loops which are β1-β2 strands and β3-β4 strands are also detected. Interestingly, the crystal structure shows the dimeric state actually. In order to make sure BC0266 has dimeric molecular weight, size-exclusion chromatography with reference proteins in the Gel Filtration Calibration Kits was conducted. Theoretical molecular weight of the *B. cereus* MazF monomer containing N-terminal His-tag is 15.1 kDa, it is reasonable that oligomeric state of *B. cereus* MazF is homodimer (30.2 kDa) as it was eluted at almost the same time as that of carbonic anhydrase (29kDa). The results of this experiment show that the oligomeric state and the molecular weight are match.

(a) Data Collection Details	
X-ray source	BL44XU beamline of Spring-8, Japan
X-ray wavelength (Å)	0.899995
Space group	$P3_121$
Unit cell parameters: *a*, *b*, *c* (Å)	60.648, 60.648, 76.247
Unit cell parameters: α, β, γ (°)	90.0, 90.0, 120.0
Resolution range (Å)	50.0-2.00
Observed reflections (>1σ)	231077
Unique reflections	21852
<I/σ(I)>	10.74 (2.97)[e]
Completeness (%)	99.3 (95.5)[e]
Multiplicity[a]	10.57 (9.76)[e]
R_{merge} (%)[b]	12.1 (47.9)[e]
$CC_{1/2}$	0.997 (0.918)[e]
(b) Refinement statistics	
R_{work}[c] (%)	18.9
R_{free}[d] (%)	22.5
No. of atoms/average *B* factor (Å²)	997/46.2
RMSD[f] from ideal geometry: Bond distance (Å)	0.008
RMSD[f] from ideal geometry: Bond angle (°)	1.108
Ramachandran statistics: Most favored regions (%)	96.49
Ramachandran statistics: Additional allowed regions (%)	3.51
PDB accession code	7BXY

Fig. 10. Structure data collection and refinement statistics

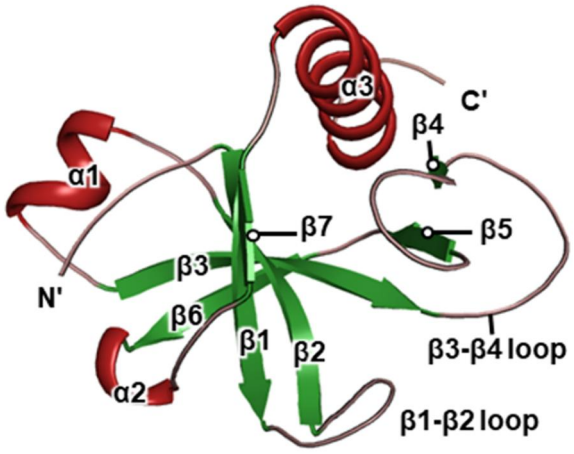

Fig. 11. Monomer structure of BC0266

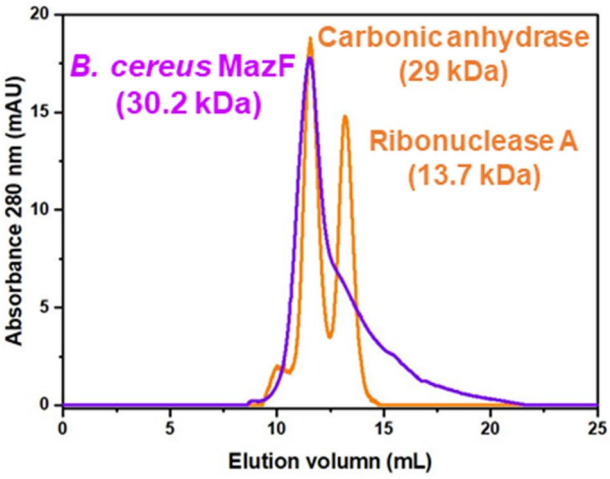

Fig. 12. Gel filtration of dimeric M.W

3.5. Comparison of *B. cereus* MazF with MazF Homologs

To relate the structural characteristics of B. cereus MazF with other MazF strucutres, sequence and structural alignment were performed. Sequence alignment were displayed with *Staphylococcus aureus*, *M.tuberculosis* MazF3, MazF4 and MazF7. Overall sequences are very similar. Especially, the results showed that two key residues of Arg25 and Thr48 are well conserved among multiple MazFs. Conserved active site residues are emphasized with star symbol in figure 13. Conserved active residues are all same except Lys19 conserved in M. tuberculosis MazF4 and Ser51 conserved in M. tuberculosis MazF7. And in terms of structural alignment, sites of the key residues are located in similar place. Comparison with other MazFs, overall structural folding is also similar.

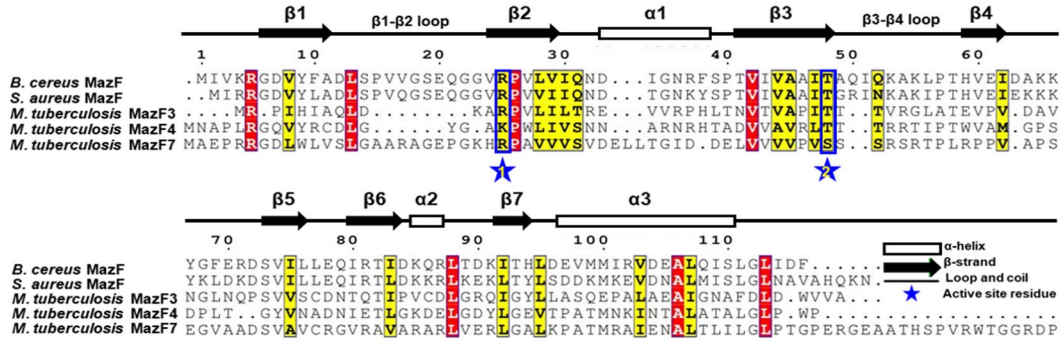

Fig. 13. Sequence alignment of B. cereus MazF with other MazFs

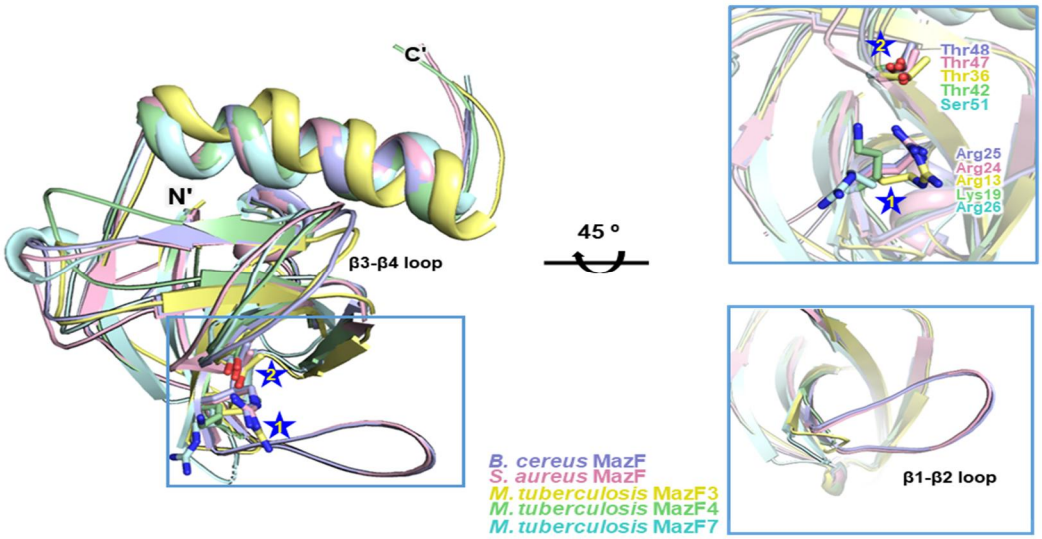

Fig. 14. Structural alignment of B. cereus MazF with other MazFs

3.6. Functional activity

MazF is a ribonuclease that is known to cleave RNA substrate with ribosome independent manner. In vitro ribonuclease activity test was performed to demonstrate of *B. cereus* MazF activity. A synthetic RNA strand which has random and unknown sequence is used as substrate. If these substrates are cleaved, they emit fluorescence in proportion to the amount of the substrates cleaved by *B. cereus* MazF. Relative fluorescence units (RFU) was greatly increased as time and dose dependency. Furthermore, two single and one double site-directed mutagenesis on the two key catalytic residues of Arg25 and Thr48 were performed. The results showed that double mutations of both Arg25 and Thr48 are more powerful to inhibit ribonuclease activity than single mutations of either Arg25 or Thr48. The last functional study was toxin-antitoxin binding test in order to make sure whether BC0266 is TA protein. TA system is that toxin and antitoxin can bind together only with each pair. This is because the residues present in antitoxin form a specific charge density for binding specific toxin. Using this, I added antitoxin without his tags and proceeded with affinity chromatography. If the two are not pairs of each other, the antitoxin does not interact with the toxin, and as a result, the untagged antitoxin does not bind to the column. But as a result, I could see that the antitoxin was refined in the column along with the toxin, and I could see that these two were TA pairs of each other's.

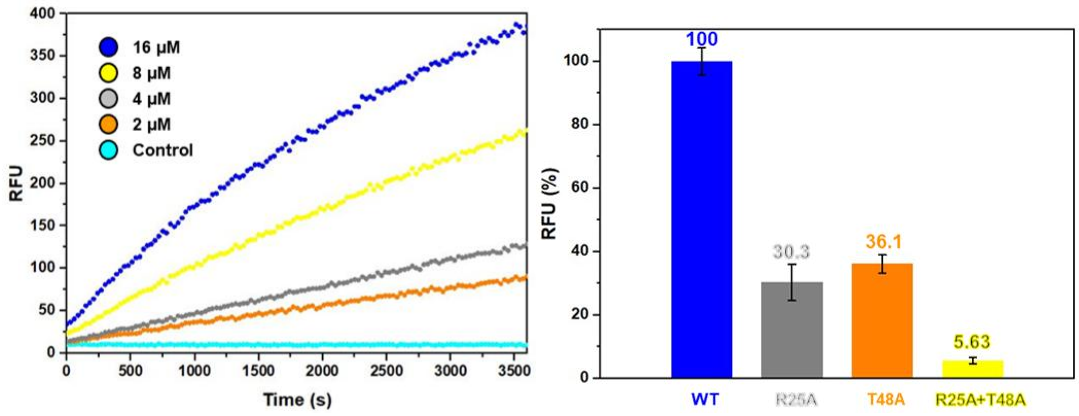

Fig. 15. In vitro assay or ribonuclease activity and mutation

V. Conclusion

I conducted an in-depth characterization and investigation on putative mRNA interferase MazF in *B. cereus*. High-resolution (2.0 Å) structure was obtained by X-ray crystallography, and overall structural folding of *B. cereus* MazF indicated β-barrel arrangement containing two independent β-sheets identical to that of MazF toxins. Through comparison analysis with previously reported structures of MazFs, amino acid residues Arg25 and Thr48 in *B. cereus* MazF were well conserved with other MazFs and were also confirmed as key residues in the catalytic activity of *B. cereus* MazF. Also, β1–β2 and β3–β4 loops were clearly observed in *B. cereus* MazF structure and their role in the recognition of target RNA substrate depending on the binding of its cognate antitoxin was discussed. From previously conducted studies, it can be presumed that the β1–β2 loop acts as a gateway to binding of its target RNA substrate. Lastly, ribonuclease activity test via in vitro assay together with site-directed mutational studies on Arg25 and Thr48 showed a decrease in its ribonuclease activity, which was consistent in other MazF toxins. Altogether, my study provides a unified structural and functional basis that mRNA interferase BC0266 is indeed a MazF toxin. This is the first determined MazF and toxin structure in type II TA system of *B. cereus*. My work may be a rational basis for understanding the TA systems regarding the stress-responsive toxin MazF and the general regulatory mechanisms of TA systems.

VI. References

1. Page, R.; Peti, W. Toxin-antitoxin systems in bacterial growth arrest and persistence. Nat. Chem. Biol. 2016, 12, 208–214, doi:10.1038/nchembio.2044.
2. Yamaguchi, Y.; Park, J.H.; Inouye, M. Toxin-antitoxin systems in bacteria and archaea. Annu. Rev. Genet. 2011, 45, 61–79, doi:10.1146/annurev-genet-110410-132412.
3. Lee, K.Y.; Lee, B.J. Structure, Biology, and Therapeutic Application of Toxin-Antitoxin Systems in Pathogenic Bacteria. Toxins 2016, 8, 305, doi:10.3390/toxins8100305.

4. Ogura, T.; Hiraga, S. Mini-F plasmid genes that couple host cell division to plasmid proliferation. Proc. Natl. Acad. Sci. USA 1983, 80, 4784–4788.

5. Pandey, D.P.; Gerdes, K. Toxin-antitoxin loci are highly abundant in free-living but lost from hostassociated prokaryotes. Nucleic Acids Res. 2005, 33, 966–976, doi:10.1093/nar/gki201.

6. Sengupta, M.; Austin, S. Prevalence and significance of plasmid maintenance functions in the virulence plasmids of pathogenic bacteria. Infect. Immun. 2011, 79, 2502–2509, doi:10.1128/IAI.00127-11.

7. Kwan, B.W.; Valenta, J.A.; Benedik, M.J.; Wood, T.K. Arrested protein synthesis increases persister-like cell formation. Antimicrob. Agents Chemother. 2013, 57, 1468–1473, doi:10.1128/AAC.02135-12.

8. Goeders, N.; Van Melderen, L. Toxin-Antitoxin Systems as Multilevel Interaction Systems. Toxins 2014, 6, 304–324, doi:10.3390/toxins6010304.

9. Mutschler, H.; Gebhardt, M.; Shoeman, R.L.; Meinhart, A. A novel mechanism of programmed cell death in bacteria by toxin-antitoxin systems corrupts peptidoglycan synthesis. PLoS Biol. 2011, 9, e1001033, doi:10.1371/journal.pbio.1001033.

10. Unoson, C.; Wagner, E.G.H. A small SOS-induced toxin is targeted against the inner membrane in Escherichia coli. Mol. Microbiol. 2008, 70, 258–270, doi:10.1111/j.1365-2958.2008.06416.x.

11. Goeders, N.; Chai, R.; Chen, B.H.; Day, A.; Salmond, G.P.C. Structure, Evolution, and Functions of Bacterial Type III Toxin-Antitoxin Systems. Toxins 2016, 8, 282, doi:10.3390/toxins8100282.

12. Lobato-Marquez, D.; Diaz-Orejas, R.; Garcia-del Portillo, F. Toxin-antitoxins and bacterial virulence. FEMS Microbiol. Rev. 2016, 40, 592–609, doi:10.1093/femsre/fuw022.

13. Harms, A.; Brodersen, D.E.; Mitarai, N.; Gerdes, K. Toxins, Targets, and Triggers: An Overview of ToxinAntitoxin Biology. Mol. Cell 2018, 70, 768–784, doi:10.1016/j.molcel.2018.01.003.

14. Wang, X.X.; Lord, D.M.; Cheng, H.Y.; Osbourne, D.O.; Hong, S.H.; Sanchez-Torres, V.;

Quiroga, C.; Zheng, K.; Herrmann, T.; Peti, W.; et al. A new type V toxin-antitoxin system where mRNA for toxin GhoT is cleaved by antitoxin GhoS. Nat. Chem. Biol. 2012, 8, 855–861, doi:10.1038/Nchembio.1062.

15. Aakre, C.D.; Phung, T.N.; Huang, D.; Laub, M.T. A Bacterial Toxin Inhibits DNA Replication Elongation through a Direct Interaction with the beta Sliding Clamp. Mol. Cell 2013, 52, 617–628, doi:10.1016/j.molcel.2013.10.014.

16. Yamaguchi, Y.; Inouye, M. mRNA interferases, sequence-specific endoribonucleases from the toxinantitoxin systems. Prog. Mol. Biol. Transl. Sci. 2009, 85, 467–500, doi:10.1016/S0079-6603(08)00812-X.

17. Aizenman, E.; Engelberg-Kulka, H.; Glaser, G. An Escherichia coli chromosomal "addiction module" regulated by guanosine [corrected] 3′,5′-bispyrophosphate: A model for programmed bacterial cell death. Proc. Natl. Acad. Sci. USA 1996, 93, 6059–6063.

18. Marianovsky, I.; Aizenman, E.; Engelberg-Kulka, H.; Glaser, G. The regulation of the Escherichia coli mazEF promoter involves an unusual alternating palindrome. J. Boil. Chem. 2001, 276, 5975–5984, doi:10.1074/jbc.M008832200.

19. Kedzierska, B.; Lian, L.Y.; Hayes, F. Toxin-antitoxin regulation: Bimodal interaction of YefM-YoeB with paired DNA palindromes exerts transcriptional autorepression. Nucleic Acids Res. 2007, 35, 325–339, doi:10.1093/nar/gkl1028.

20. Brantl, S.; Muller, P. Toxin(-)Antitoxin Systems in Bacillus subtilis. Toxins 2019, 11, 262, doi:10.3390/toxins11050262.

21. Leplae, R.; Geeraerts, D.; Hallez, R.; Guglielmini, J.; Dreze, P.; Van Melderen, L. Diversity of bacterial type II toxin-antitoxin systems: A comprehensive search and functional analysis of novel families. Nucleic Acids Res. 2011, 39, 5513–5525, doi:10.1093/nar/gkr131.

22. Anantharaman, V.; Aravind, L. New connections in the prokaryotic toxin-antitoxin network: Relationship with the eukaryotic nonsense-mediated RNA decay system. Genome Biol. 2003, 4, R81, doi:10.1186/gb-2003- 4-12-r81

23. Schifano, J.M.; Edifor, R.; Sharp, J.D.; Ouyang, M.; Konkimalla, A.; Husson, R.N.; Woychik, N.A. Mycobacterial toxin MazF-mt6 inhibits translation through cleavage of 23S rRNA at the ribosomal A site. Proc. Natl. Acad. Sci. USA 2013, 110, 8501–8506, doi:10.1073/pnas.1222031110.

24. Ehling-Schulz, M.; Lereclus, D.; Koehler, T.M. The Bacillus cereus Group: Bacillus Species with Pathogenic Potential. Microbiol. Spectr. 2019, 7, doi:10.1128/microbiolspec.GPP3-0032-2018.

25. Bottone, E.J. Bacillus cereus, a volatile human pathogen. Clin. Microbiol. Rev. 2010, 23, 382–398, doi:10.1128/CMR.00073-09.

26. Fernandez-Garcia, L.; Blasco, L.; Lopez, M.; Bou, G.; Garcia-Contreras, R.; Wood, T.; Tomas, M. ToxinAntitoxin Systems in Clinical Pathogens. Toxins 2016, 8, 227, doi:10.3390/toxins8070227.

27. Krissinel, E.; Henrick, K. Inference of macromolecular assemblies from crystalline state. J. Mol. Biol. 2007, 372, 774–797, doi:10.1016/j.jmb.2007.05.022.

28. Zorzini, V.; Buts, L.; Sleutel, M.; Garcia-Pino, A.; Talavera, A.; Haesaerts, S.; De Greve, H.; Cheung, A.; van Nuland, N.A.; Loris, R. Structural and biophysical characterization of Staphylococcus aureus SaMazF shows conservation of functional dynamics. Nucleic Acids Res. 2014, 42, 6709–6725, doi:10.1093/nar/gku266.

29. Hoffer, E.D.; Miles, S.J.; Dunham, C.M. The structure and function of Mycobacterium tuberculosis MazFmt6 toxin provide insights into conserved features of MazF endonucleases. J. Biol. Chem. 2017, 292, 7718– 7726, doi:10.1074/jbc.M117.779306.

30. Chen, R.; Tu, J.; Liu, Z.; Meng, F.; Ma, P.; Ding, Z.; Yang, C.; Chen, L.; Deng, X.; Xie, W. Structure of the MazF-mt9 toxin, a tRNA-specific endonuclease from Mycobacterium tuberculosis. Biochem. Biophys. Res. Commun. 2017, 486, 804–810, doi:10.1016/j.bbrc.2017.03.132.

31. Simanshu, D.K.; Yamaguchi, Y.; Park, J.H.; Inouye, M.; Patel, D.J. Structural basis of mRNA recognition and cleavage by toxin MazF and its regulation by antitoxin MazE in Bacillus subtilis. Mol. Cell 2013, 52, 447–458, doi:10.1016/j.molcel.2013.09.006.

32. Zorzini, V.; Mernik, A.; Lah, J.; Sterckx, Y.G.; De Jonge, N.; Garcia-Pino, A.; De Greve, H.; Versees, W.; Loris, R. Substrate Recognition and Activity Regulation of the Escherichia coli mRNA Endonuclease MazF. J. Biol. Chem. 2016, 291, 10950–10960, doi:10.1074/jbc.M116.715912.

33. Kamada, K.; Hanaoka, F.; Burley, S.K. Crystal structure of the MazE/MazF complex: Molecular bases of antidote-toxin recognition. Mol. Cell 2003, 11, 875–884, doi:10.1016/s1097-2765(03)00097-2.

34. Guillen Schlippe, Y.V.; Hedstrom, L. A twisted base? The role of arginine in enzyme-catalyzed proton abstractions. Arch. Biochem. Biophys. 2005, 433, 266–278, doi:10.1016/j.abb.2004.09.018.

35. Dunican, B.F.; Hiller, D.A.; Strobel, S.A. Transition State Charge Stabilization and Acid-Base Catalysis of mRNA Cleavage by the Endoribonuclease RelE. Biochemistry 2015, 54, 7048–7057, doi:10.1021/acs.biochem.5b00866.

36. Gogos, A.; Mu, H.; Bahna, F.; Gomez, C.A.; Shapiro, L. Crystal structure of YdcE protein from Bacillus subtilis. Proteins 2003, 53, 320–322, doi:10.1002/prot.10457.

37. Kang, S.M.; Kim, D.H.; Jin, C.; Lee, B.J. A Systematic Overview of Type II and III Toxin-Antitoxin Systems with a Focus on Druggability. Toxins 2018, 10, 515, doi:10.3390/toxins10120515.

38. Cook, G.M.; Robson, J.R.; Frampton, R.A.; McKenzie, J.; Przybilski, R.; Fineran, P.C.; Arcus, V.L. Ribonucleases in bacterial toxin-antitoxin systems. Biochim. Biophys. Acta 2013, 1829, 523–531, doi:10.1016/j.bbagrm.2013.02.007.

39. Kang, S.M.; Kim, D.H.; Lee, K.Y.; Park, S.J.; Yoon, H.J.; Lee, S.J.; Im, H.; Lee, B.J. Functional details of the Mycobacterium tuberculosis VapBC26 toxin-antitoxin system based on a structural study: Insights into unique binding and antibiotic peptides. Nucleic Acids Res. 2017, 45, 8564–8580, doi:10.1093/nar/gkx489.

40. Kim, D.H.; Kang, S.M.; Park, S.J.; Jin, C.; Yoon, H.J.; Lee, B.J. Functional insights into the Streptococcus pneumoniae HicBA toxin-antitoxin system based on a structural study. Nucleic Acids Res. 2018, 46, 6371– 6386, doi:10.1093/nar/gky469.

41. Adams, P.D.; Afonine, P.V.; Bunkoczi, G.; Chen, V.B.; Davis, I.W.; Echols, N.; Headd, J.J.; Hung, L.W.; Kapral, G.J.; Grosse-Kunstleve, R.W.; et al. PHENIX: A comprehensive Python-based system for macromolecular structure solution. Acta Crystallogr. D Biol. Crystallogr. 2010, 66, 213–221, doi:10.1107/S0907444909052925.

42. Emsley, P.; Lohkamp, B.; Scott, W.G.; Cowtan, K. Features and development of Coot. Acta Crystallogr. D Biol. Crystallogr. 2010, 66, 486–501, doi:10.1107/S0907444910007493.

43. Brunger, A.T. Free R value: A novel statistical quantity for assessing the accuracy of crystal structures. Nature 1992, 355, 472–475.

45. Chen, V.B.; Arendall, W.B.; Headd, J.J.; Keedy, D.A.; Immormino, R.M.; Kapral, G.J.; Murray, L.W.; Richardson, J.S.; Richardson, D.C. MolProbity: All-atom structure validation for macromolecular crystallography. Acta Crystallogr. D Biol. Crystallogr. 2010, 66, 12–21, doi:10.1107/S0907444909042073.

47. Thompson, J.D.; Higgins, D.G.; Gibson, T.J. CLUSTAL W: Improving the sensitivity of progressive multiple sequence alignment through sequence weighting, position-specific gap penalties and weight matrix choice. Nucleic Acids Res. 1994, 22, 4673–4680, doi:10.1093/nar/22.22.4673.

48. agrilinks.org/sites/default/files/6.20.18_master_deck_2.pdf.

49. Sung-Min Kang, Ji Sung Koo, Chang-Min Kim, Do-Hee Kim and Bong-Jin Lee 1; mRNA Interferase Bacillus cereus BC0266 Shows MazF-Like Characteristics Through Structural and Functional Study Toxins 2020, 12, 380.

50. Jin Chenglong Structure and Functional Study on HigBA from Streptococcus pneumoniae

국문초록

Toxin-Antitoxin(TA) 시스템은 박테리아에 만연하며 스트레스에 반응하여 세포의 성장을 조절한다. TA system에 관련되서 다양한 기능이 알려짐에 따라 그 중요성이 점차 부각되고 있는 추세이다. 여기서 우리는 mRNA interferase의 기능을 가지는 BC0266의 크리스탈 구조를 보여주고 그것을 typeII 톡신 MazF라고 부른다. MazF 톡신은 스트레스 상황에서 ribonuclease 기능이 활성화되는데 이는 ribosome-independent하게 그리고 sequence-specific하게 작용한다. 이것의 지속적인 활동은 독성결과를 유발하고 결국 박테리아 사멸로 이어진다. 이 연구에서 바실러스 세레우스에서 유래한 MazF의 구조와 기능 연구를 했으며 최초로 바실러스 세레우스의 MazF 톡신 구조를 구했다. 특히 바실러스 MazF는 PemK와 같은 fold와 유사성을 지니며 RNA-substrate recognizing loop을 가지고 있는데 이는 매우 높은 resolution으로 관측되었다. 바실러스 세레우스의 MazF 주요 잔기는 촉매활성을 가지고 있으며 mutation 실험을 통해 in vitrto assay를 진행한 결과 이 잔기들이 ribonucleic activity를 가지고 있고 celluar toxicity에 매우 중요한 인자들이라는 것을 알 수 있었다.

주요어: Toxin-Antitoxin system, MazF type II toxin, *Bacillus cereus,* mRNA interferase, X-ray crystallography

Student number: 2019-24434